A stochastic individual-based model for the growth of a stand of Japanese knotweed including mowing as a management technique.

François Lavallée[1,2,*], Charline Smadi[1,2], Isabelle Alvarez[1,2], Björn Reineking[3], François-Marie Martin[3], Fanny Dommanget[3], Sophie Martin[1,2],

Abstract

Invasive alien species are a growing threat for the environment and health. They also have a major economic impact, as they can damage many infrastructures. The Japanese knotweed (*Fallopia japonica*), present in North America, Northern and Central Europe as well as in Australia and New Zealand, is listed by the World Conservation Union as one of the world's worst invasive species. So far, most models have dealt with the knotweed invasion without management. This paper aims to provide a model able to study and predict the dynamics of a stand of Japanese knotweed taking into account mowing as a management technique. The model is stochastic and individual-based, which allows us to take into account the behaviour of individuals depending on their size and location, as well as individual stochasticity. We set plant dynamics parameters based on a calibration with field data and studied the influence of the initial population size, the mean number of mowing events a year and the management project duration on the mean area and mean number of crowns. The results provide the sets of parameters for which it is possible to obtain stand eradication, and the minimum duration of the management project necessary to achieve this.

Keywords: Invasive plant, *Fallopia spp.*, *Reynoutria spp.*, *Polygonum spp.*, individual-based model, management strategies, dynamics, model exploration

1. Introduction

Invasive alien species are a growing problem for the environment and human health. They may cause a loss of biodiversity (Murphy and Romanuk, 2014), changes in ecosystem functioning (Strayer, 2012) or affect human well-being (Shackleton et al., 2019). They also have a major economic impact (Kettunen et al., 2009; Pimentel et al., 2005). The need to act against invasive species is based on their global and local impacts as well as international policy engagements. For example, since 1992, the Convention on Biological Diversity (article 8[4]) compels the parties to "prevent the introduction of, control or eradicate those alien species which threaten ecosystems, habitats or species". Managing invasive species is a global and local challenge and management strategies depend on species, the stage of the invasion process and the scale of action (Simberloff et al., 2013; Hui and Richardson, 2017).

Many studies focus on optimal management of invasive species (Baker and Bode, 2016; Harris et al., 2009; Travis et al., 2011). A frequent question in the literature of invasive species management through mathematical modelling is to assess the benefit of a spatial prioritization of management activities. For example, for seed dispersal species, is it more profitable to remove the individuals at the heart of the invasion or those on the periphery (Harris et al., 2009)? Another issue discussed in the literature of invasive species management is the temporal distribution of actions. For example, we know that early detection and a rapid response to the invasion may be more efficient (Pyšek and Richardson, 2010). As such, questions related to detectability strategies may help to optimize containment actions and early eradication of newly arrived individuals (Cacho et al., 2007, 2010). However, management programs frequently start when the species is already well established. In that situation, what is needed in terms of time and cost to achieve eradication? Panetta et al. (2011) developed a model to study the feasibility of eradicating the invasive species studied. Cacho et al. (2007) and Hester et al. (2010) also addressed this question, integrating management costs (administration, search, control and travel) and proposed a population model for the growth of invasive species. Moreover, when the eradication is no longer attainable, management objectives may then switch to containment of the invasive species. For a given landscape Bonneau et al. (2019) proposed an optimal search and destroy strategy which takes into account visit cost, removal cost and presence probability. When dynamics are considered, crucial questions would then concern the trade-off between intensity and length of the control strategy to maintain the invasion under a desirable threshold. For instance, is it better to act significantly at the beginning of the management project and then to control the invasion with a lower investment (as in Meier et al. (2014)),

*Corresponding author
Email address: francois.lavallee@irstea.fr (François Lavallée)
[1]IRSTEA UR LISC, Laboratoire d'ingénierie pour les Systèmes Complexes, 9 avenue Blaise-Pascal CS 20085, 63178 Aubière, France
[2]Complex Systems Institute of Paris Île-de-France, 113 rue Nationale, 75013, Paris, France
[3]Univ. Grenoble Alpes, Irstea, LESSEM, 38000 Grenoble, France
[4]https://www.cbd.int/convention/articles/default.shtml?a=cbd-08

or to have a longer management project that requires a less intense effort? This trade-off between intensity and length of the control strategy is the crucial question we address in this article in the case of the Japanese knotweed.

Actually, among the worst invasive species threatening biodiversity, Asian knotweeds raise particular management issues. This complex of three species (the Japanese knotweed, *Fallopia japonica* [Houtt.] Ronse Decraene, the giant knotweed, *Fallopia sachalinensis* [Schmidt Petrop.] Ronse Decraene and the hybrid between these two plants, the Bohemian knotweed (*Fallopia* × *bohemica* Chrtek & Chrtkova) have invaded Europe and North America. Native to Eastern Asia, knotweeds were introduced for ornamental purposes at the end of the 19th century (Bailey and Wisskirchen, 2006; Barney et al., 2006; Beerling et al., 1994). They are also present in Australia, New Zealand and Chile (Alberternst and Böhmer, 2006; Saldaña et al., 2009).

Asian knotweeds quickly invade the environment in which they grow (Gowton et al., 2016) and have large impacts (Lavoie, 2017). They displace other plant species through light competition and allelopathy (Dommanget et al., 2014; Siemens and Blossey, 2007), affect native fauna diversity (Abgrall et al., 2018; Gerber et al., 2008; Maerz et al., 2005; Serniak et al., 2017) and modify ecosystem functioning (Dassonville et al., 2011; Tharayil et al., 2013). In addition, the control costs are very high, estimated at U.S.$ 250 million a year in Great Britain (Colleran and Goodall, 2014) and more than 2 billion euros a year in Europe (Kettunen et al., 2009).

Asian knotweeds grow in a wide variety of soils: sandy, swampy and rocky. They mainly invade human-modified habitats such as roadsides, waste dumps, but also river banks. They are perennial geophytes: their rhizomes allow them to spend the winter season buried in the ground (De Waal, 2001). Their rhizomes also play a major role in their propagation, thanks to their strong regeneration capacity (Bailey et al., 2009; Brock et al., 1992). Once arrived in a new area, the rhizome expands centrifugally and a new stand can sustainably establish in a few weeks (Gowton et al., 2016; Smith et al., 2007).

Once established and due to their extensive rhizome network, Asian knotweeds are extremely hard to remove. Rhizomes account for two-thirds of their biomass (Barney et al., 2006) and can expand several metres away from the visible invasion front (Barney et al., 2006). The resources they store can be efficiently remobilized after mowing events (Rouifed et al., 2011). Some authors estimate that six cuttings are needed to significantly reduce belowground biomass (Gerber et al., 2010). Understanding the underground development of Asian knotweeds is therefore crucial to gain insight into their local propagation and performance. Moreover, it could help if more efficient management were designed.

Since underground organs are almost inaccessible to observers, direct observations are scarce and models could help to approach their dynamics and provide a better understanding of how management actions can affect their development. To our knowledge, there are very few models in the literature that describe the growth of a Japanese knotweed stand, and among them, rare are those that include a management technique.

In Smith et al. (2007), the authors built a 3D correlated random walk model of the development of the subterranean rhizome network for a single stand of Japanese knotweed. Their model was based on knowledge of the morphology and physiology of the plant. They studied the model through simulations and they observed a quadratic expansion of the area invaded.

Dauer and Jongejans (2013) proposed an "Integral Projection Model", inspired from matrix population models, for the plant dynamics at the stand level. The variable of interest was a continuous variable which stands for the height or the total biomass of the plant, and the authors used a simplified plant life cycle to model the transition between states, such as the transition from new shoots to crown (a crown is the location of a terminal bud from which stems emerge). They studied the parameters that have the largest effect on the growth rate of the population.

Gourley et al. (2016) developed a mathematical model for biocontrol of *Fallopia japonica* using one of its co-evolved natural enemies, the Japanese sap-sucking psyllid *Aphalara itadori*. It is a deterministic model that describes the dynamics of the number of insects (larvae and adults), the total weight of the knotweed stems and the rhizome biomass. Two key parameters of their model are the time it takes a larva to consume and digest the sap from the plant stems, and the duration of the larval stage (Landi et al., 2018).

A commonly used management technique for Asian knotweed stands is mowing. Managers can vary the intensity and frequency, which motivates a study of the effects of these two parameters on the stand dynamics. This paper aims at examining the influence of mowing on the growth of an Asian knotweed stand. More precisely, we studied the influence of the initial population size, the mean number of mowing events a year and the management project duration on the mean area and number of crowns of the stands. To our knowledge, existing models have not been designed to study such questions. We adopt a stochastic formalism enabling us to study the early stage of invasion when the mean field approximation is not valid. Indeed mean field approximation requires the presence of many individuals and thus the species to be present for a long time. The description of phenomena at the individual level enabled us to take into account the variability between crowns, for example due to different ages.

The paper is organized as follows. Section 2 is devoted to the description of the ecological mechanisms under consideration (apical dominance, intraspecific competition, etc.), the presentation of the mathematical model, as well as the methods. The results are presented in Section 3. In particular, we calibrated the plant dynamics with field data collected in the French Alps. Numerical simulations were carried out with OpenMOLE software (Reuillon et al., 2013) to study the influence of management parameters on the population growth. Finally, we summarize our results and discuss their implications and shortcomings in Section 4.

2. Materials and methods

In this section we provide a description of the dynamical model for the growth of a stand of Japanese knotweed includ-

ing mowing as a management technique. We also describe the methods used to study this through numerical simulations.

In the following, the term "individual" will refer to crowns. We recall that a crown is the location of a terminal bud from which stems emerge. Individuals are characterized by their position x in the plane and their underground biomass a (i.e. the biomass rhizome connected to the crown, referred to as biomass).

The following notations will be used to describe our model:

- $\chi := \mathbb{R}^2 \times \mathbb{R}_+$, is the state space of positions and biomasses. In the model, a crown is represented by a Dirac mass $\delta_{(x,a)}$, with $(x, a) \in \chi$, where x stands for the position of the crown and a is the biomass associated with the crown.

- The set of crowns present at time t is described by the measure $Z_t \in \mathcal{M}(\chi)$, where $\mathcal{M}(\chi)$ is the set of finite point measures on χ whose masses of points are 0 or 1.

$$\mathcal{M}(\chi) := \left\{ \sum_{i=1}^{n} \delta_{(x_i,a_i)} \ , \ n \geq 0, \ (x_1, a_1), \ldots, (x_n, a_n) \in \chi \right\}.$$

Using $\mathcal{M}(\chi)$ allows us not to set *a priori* the number of individuals in the model, since it contains all the possible population sizes.

2.1. Description of the phenomena included in the model

Birth: An individual with trait $(x, a) \in \chi$ (i.e. its position is x and it has a biomass a) gives birth at rate $b(x, Z)$, where $Z \in \mathcal{M}(\chi)$ describes the state of the population (i.e. the positions and biomasses of all individuals). We assume that this birth rate does not depend on an individual's biomass a. A crown can give birth to at most two daughter crowns (Smith et al., 2007) at a rate depending on the neighbouring individuals present at a distance less than *distanceParent*. Hence, if a crown has already given birth to two daughters (in fact if there are already three individuals at a distance shorter than *distanceParent* from it since we count its parent), it has a null birth rate (it no longer gives birth). We will see in the next section that a daughter crown can in principle be at a distance greater than *distanceParent* from its parent. This phenomenon may be balanced by the fact that crowns from another parent can be at a distance less than *distanceParent*. These functioning rules allow us to account for the effects of apical dominance: if a crown dies, the apical dominance it exerts on the neighbouring lateral buds ceases, and they may develop to form aerial shoots and create a new crown.

Bashtanova et al. (2009), Adachi et al. (1996) and Dauer and Jongejans (2013) mention this phenomenon of apical dominance in a general way, but they do not quantify it. That is why we will use a calibration method to set its value (in fact we use this method for all parameters, see Section 2.4).

The rate at which an individual with position x gives birth can thus be expressed as follows:

$$b(x, Z) = \bar{b}_{\{\sum_{y \in V(Z)} 1_{\{\|x-y\| \leq distanceParent\}} \leq 3\}}, \tag{1}$$

where $\|.\|$ denotes the usual norm on $\mathbb{R}^2$, $\bar{b}$ is the maximum birth rate (under ideal conditions) and

$$V(Z) := \{x \in \mathbb{R}^2, Z(\{x\} \times \mathbb{R}_+) > 0\} \tag{2}$$

is the set of the positions of the crowns present in the population Z.

Dispersal of the newborn individual: An individual with trait (x, a) which gives birth generates an individual at position x'. Here we choose a Gamma law for the birth distance distribution. Its density on $\mathbb{R}^+$ is given by

$$x \mapsto 1/(scale^{shape}\Gamma(shape))x^{(shape-1)}e^{-(x/scale)}. \tag{3}$$

The parameters ($shape$, $scale$) of the distribution will be subject to calibration. We assume a uniform distribution on $x' - x$ direction angle to the x-axis.

Moreover, we will model the phenomenon of intra-specific competition by considering that an individual is really born only if it does not fall too close to an already existing crown. So we introduce the set C depending on the population state Z and the position of the potential parent x:

$$C_{x,Z} := \{z \in \mathbb{R}^2, \ \forall y \in V(Z) \backslash \{x\}, \ \|y - z\| > distanceCompetition\}. \tag{4}$$

The newborn individual must therefore be at a distance greater than *distanceCompetition* from its neighbours not to fall in the zone of intra-specific competition. This principle of excluded zones (for the birth of an individual) is also used in Smith et al. (2007): the areas around the crowns are subject to competition for light and the emergence of new crowns is not allowed.

The diagram in Figure 1 shows distances playing a role during a birth event.

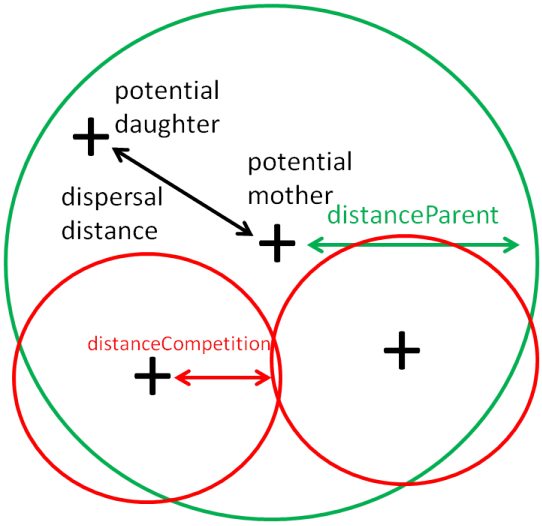

Figure 1: Diagram representing a birth event. A cross stands for a crown position. We also indicate the different distances used in the model.

Biomass dynamics: In Seiger et al. (1997), the authors present the effects of mowing on rhizome growth. They find that rhizome biomass increases significantly throughout the growing season, unlike above-ground biomass, which stops growing significantly at the end of the summer. If the aerial shoots are not cut, the growth of the underground biomass a is assumed to evolve according to a Von Bertalanffy's law (Paine et al., 2012), presented below (Equation (6)). How mowing aerial shoots impacts the rhizome development is poorly known. We assume that mowing results in a decrease of underground biomass. This assumption stems from the use of rhizome resources for aerial shoot regeneration (see Gerber et al. (2010)). In Rouifed et al. (2011), the authors also note that mowing impacts the amount of underground biomass at the end of the season, and induces a decreasing rhizome density with depth (whereas without mowing it is constant). However, we do not take this phenomenon into account, since the model is planar.

Mowing events occur at a rate $1/\tau$ (there is thus on average τ mowing events a year), and a proportion $proportionMowing$ (constant) of individuals is mown.

After a mowing event, it is assumed that the underground biomass a of an individual is immediately impacted and becomes $a * F(a)$, where F takes values in $[0, 1]$ and describes the mowing effect as a function of the individual biomass. In order to take into account the fragility of young crowns, the function F describing the impact of mowing on biomass is assumed to be higher for low biomasses (we therefore take F increasing, which implies that for two biomasses $a_1 < a_2$, we will have $a_1 * F(a_1) < a_2 * F(a_2)$). We assume that F is expressed as:

$$\forall a \in \mathbb{R}_+,\ F(a) = 1 - exp(-mowingParameter * a), \qquad (5)$$

where $mowingParameter$ is a parameter that acts on the decay rate of the exponential function.

For the biomass growth of a crown when there is no mowing, we use Von Bertalanffy's Equation (6). First described in von Bertalanffy (1934), this equation has been widely used in forestry (Zeide, 1993). Here, it describes the dynamics of the biomass as a function of time. It is based on simple physiological arguments: the growth rate of the organism decreases with biomass.

$$\frac{da(t)}{dt} = L(K - a(t)) =: v(a(t)), \qquad (6)$$

where L is the growth rate at low biomass and K is the maximum asymptotic biomass. If we assume that the biomass at time t_0 is equal to a_0, then for all $t \geq t_0$, we obtain:

$$a(t) = a_0 e^{-L(t-t_0)} + K(1 - e^{-L(t-t_0)}). \qquad (7)$$

Moreover, we assume that all crowns are born with the same biomass $a_0 \in \mathbb{R}_+$.

Mortality: We assume that the mortality rate is independent of the individual position. An individual alive at time t and with biomass $a(t)$ dies at a rate $m(a(t))$. We assume that the mortality m is a decreasing function of the biomass: an individual with a low biomass, either because it was just born or because it has been mown, has a higher mortality rate. So if T_0 is the time at which an individual born at time 0 dies, and whose biomass up to time t is given by the function a (we assume it is not mown), we obtain:

$$\mathbb{P}(T_0 \geq t) = e^{-\int_0^t m(a(s))\ ds}. \qquad (8)$$

In Smith et al. (2007), the authors set the probability that a segment of rhizome dies over a 4-month period (a time step in their model) to 0.0083. When there is no mowing, mortality events for crowns rarely occur in nature, explaining why the value proposed in Smith et al. (2007) is low. Having a good estimate for this value requires a sufficiently large number of observations; thus calibration is very useful to estimate a value for this type of parameter. We assume that m, the function that describes the mortality rate of a crown according to its biomass, is expressed as:

$$m(a) = deathParameterScaling\ e^{-\text{deathParameterDecrease} * a}. \qquad (9)$$

Equation (9) involves two parameters: $deathParameterDecrease$, which influences the decay rate of the function and $deathParameterScaling$ which allows one to choose the mortality rate for individuals with low biomass.

Mowing: We consider two possibilities for choosing the crowns to be mown. The first one consists in choosing the mown crowns uniformly at random (random management technique). The proportion can thus represent different qualities of mowing if the aim is to mow the whole stand depending on the tools used (by hand, brush cutter). We consider this technique when we write the mathematical formalism of the model in Section 2.2 and for the analysis of the influence of the model's parameters in section 3.2. The second one is mowing one side of the stand: it consists in determining an abscissa at the right of which every crown is mown, and at the left of which no crown is mown (side management technique). It reflects for example the case of a stand located on two plots, owned by different persons, one who manages the stand, whereas the other does not. This situation occurs frequently along roadsides. We use this management technique in the model for the calibration due to the characteristics of our data set.

We summarize the model parameters in Appendix A. There are two types: management parameters and plant dynamics parameters.

2.2. Mathematical formalism associated with the model

The class of stochastic individual-based models we are extending in this work was introduced by Bolker and Pacala (1997), and by Dieckmann et al. (2000). A rigorous probabilistic description and study was then conducted by Fournier and Méléard (2004). Since then, these models have been widely studied and extended (for instance in Champagnat (2006); Champagnat et al. (2006); Costa et al. (2016); Coron et al. (2018)).

The model proposed here and its mathematical study are drawn from the work of Tran (2006, 2008). In particular, the notations and techniques were derived from these papers.

The stochastic differential equation (10)

$$\begin{array}{ll} Z_t = \sum_{i=1}^{N_0} & \delta_{(X_i(Z_0),A_b(t,0,A_i(Z_0)))} \\ + \int_{[0,t]\times\mathbb{N}^*\times\mathbb{R}_+\times\mathbb{R}^2} & 1_{\{i\leq N_{s^-}\}}\delta_{(X_i(Z_s)+z,A_b(t,s,a_0))}1_{\{\theta\leq b(X_i(Z_s),Z_s)\}} \\ & 1_{\{X_i(Z_s)+z\,\in\, C_{X_i(Z_s),Z_s}\}}M_1(ds,di,d\theta,dz) \\ + \int_{[0,t]\times[0,1]^{N^*}} & \sum_{i=1}^{N_{s^-}} 1_{\{y_i\leq proportionMowing\}}\,(\delta_{(X_i(Z_s),A_b(t,s,A_i(Z_{s^-})*F(A_i(Z_{s^-}))))} \\ & -\delta_{(X_i(Z_s),A_b(t,s,A_i(Z_s)))})M_2(ds,dy) \\ - \int_{[0,t]\times\mathbb{N}^*\times\mathbb{R}_+} & 1_{\{i\leq N_{s^-}\}}1_{\{\theta\leq m(A_i(Z_s))\}}\delta_{(X_i(Z_s),A_b(t,s,A_i(Z_s)))}M_3(ds,di,d\theta) \end{array} \tag{10}$$

describes the plant population dynamics. It is governed by three independent Poisson random measures, defined as follows:

- $M_1(ds, di, d\theta, dz)$ is a Poisson random measure on $\mathbb{R}_+ \times \mathbb{N}^* \times \mathbb{R}_+ \times \mathbb{R}^2$ with intensity $ds \otimes n(di) \otimes d\theta \otimes D(dz)$, where $n(di)$ stands for the counting measure on $\mathbb{N}^*$ and D is the density of the law for the dispersal of a child. The measure M_1 describes the birth events.
- $M_2(ds, dy)$ is a Poisson random measure on $\mathbb{R}_+ \times [0,1]^{\mathbb{N}^*}$ with intensity $1/\tau\, ds \otimes \mathcal{U}^{\mathbb{N}^*}([0,1])$, where $\mathcal{U}([0,1])$ is the uniform law on $[0,1]$. We denote $y = (y_1, y_2, \ldots)$ for $y \in [0,1]^{\mathbb{N}^*}$. The measure M_2 describes the mowing events.
- $M_3(ds, di, d\theta)$ is a Poisson random measure on $\mathbb{R}_+ \times \mathbb{N}^* \times \mathbb{R}_+$ with intensity $ds \otimes n(di) \otimes d\theta$, where $n(di)$ stands for the counting measure on $\mathbb{N}^*$. The measure M_3 describes the death events.

In Equation (10),

$$Z_t = \sum_{i=1}^{N_t} \delta_{(X_i(Z_t),A_i(Z_t))}$$

is thus the measure that describes the population at time $t \geq 0$, A_b is the flow of the differential equation describing the dynamics of the biomass of a crown (Equation (7)). X_i (resp. A_i) denotes the position (resp. biomass) of the i-th individual in the population (in lexicographical order). Let functions $b : (x, Z) \in \mathbb{R}^2 \times \mathcal{M}(\chi) \mapsto b(x, Z)$ and $m : a \in \mathbb{R}_+ \mapsto m(a)$ be, respectively, individual birth and death rates. The application

$$C : Z \in \mathcal{M}(\chi) \mapsto C_{X_i(Z),Z} \in \mathcal{P}(\mathbb{R}^2),$$

where $\mathcal{P}(\mathbb{R}^2)$ is the set of all subsets of $\mathbb{R}^2$, gives the admissible region for the births of new individuals, which is related to intra-specific competition. The function $F : [0, K] \to [0, 1]$ models the effect of mowing crowns and τ is the average number of mowing events a year.

The first term in Equation (10) refers to the growth of the initial population: the individual biomasses increase according to the flow A_b. The second term refers to birth events. A birth event consists in choosing a potential parent and checking whether it satisfies the conditions to give birth: this is the role of the indicator functions. If it occurs, we add a Dirac mass corresponding to a new individual in the population with initial biomass a_0. The middle integral term refers to the mowing event after which an individual is replaced by another individual with the same position and a reduced biomass. The last term refers to death events, for which we delete an individual in the population subtracting a Dirac mass.

Under boundary conditions over the birth and death rates (recall that $\bar{b}$ is the upper bound of b), we have the following result obtained in a similar way as in (Tran, 2006), Propositions 2.2.5 and 2.2.6: if $Z_0 \in \mathcal{M}(\chi)$, the stochastic differential equation admits a unique pathwise strong solution $(Z_t)_{t\in\mathbb{R}_+} \in \mathbb{D}(\mathbb{R}_+, \mathcal{M}(\chi))$ such that for all $T > 0$, the number of individuals at time $t \leq T, N_t := \langle Z_t, 1\rangle = \int_{\mathbb{R}^2\times\mathbb{R}} Z_t(dx, da)$ satisfies:

$$\mathbb{E}[\sup_{t\in[0,T]} N_t] < \mathbb{E}[N_0]e^{\bar{b}T} < \infty.$$

This gives an upper bound to the growth of the population when there is no management.

2.3. Simulation of the model

The algorithm used to simulate a solution of the stochastic differential equation (10) is presented in Appendix B. To illustrate the dynamics of the stand under our model, we use Scala software (version 2.11.12). We use OpenMOLE software (Reuillon et al. (2013), version 8.0) to perform the model exploration. Finally, we use R software (version 3.4.4) for the statistical analysis of model outputs. Simulations were performed on the European Grid Infrastructure (http://www.egi.eu/).

Figure 2 displays an illustrative example of the population size dynamics (number of crowns) of one trajectory of the model, for given parameters of the plant dynamics and management parameters. The initial population size was set to 1000, the mean number of mowing events a year $\tau = 3$, the management project duration $T = 4$ years and the proportion of mown crowns $proportionMowing = 0.9$. We thus have a mean number of mowing events equal to $3 * 4 = 12$ (there were 11 in the simulation). The final population size is equal to 619, so the management strategy leads to a reduction of roughly one-third in population size.

2.4. Calibration data

Our goal is to find the influence of management parameters on the stand dynamics. We must therefore set the parameters of the plant dynamics. For some of the parameters, we could not find values in the literature. We therefore proceed to a calibration to find parameter values with which the model best reproduces the field data.

The field data are those used by Martin et al. (2018). The authors studied the invasion potential of the Japanese knotweed along an elevational gradient (i.e. in mountains), by identifying the determinants of its spatial dynamics. The experiment consists in collecting data on 19 stands of Japanese knotweed at different altitudes in the French Alps. The measurements were taken in 2008 and 2015, on the stands themselves (outline, stem density) as well as on biotic and abiotic variables. Stands were

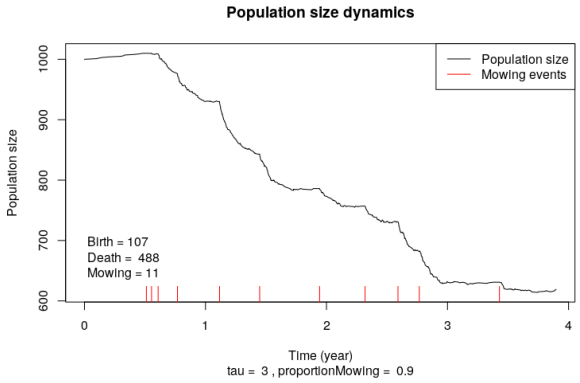

Figure 2: Illustrative example: simulation of one trajectory of the model (Equation (10)) with $\tau = 3$, $initialPopSize = 1000$, $T = 4$ and $proportionMowing = 0.9$ with plant dynamics parameters from Table 1. The black line shows the population size, red lines indicate mowing event dates.

mown or not, and for each stand, we have access to information on the management technique used by the land owner: the frequency of mowing and an estimation of the proportion of the mown stand, which corresponds to the side management technique. There is a high variability in the stands observed, both in size (from less than 2 m^2 to 350 m^2) and land conditions in which they grow such as soil quality, proximity of river, road, forest and abandoned land.

In model outputs, we compute the final and initial population sizes and areas (the area of the stand is the area of the convex hull formed around the simulated stands). From Martin et al. (2018), we use data on stand areas and crown densities so we can deduce the population size, for stands in 2008 and 2015.

As mentioned in Appendix B, the simulation operation for a stand takes place in two stages: first, the creation of the initial population given a population size to reach (we chose the size of a stand in 2008), then its dynamics, according to the information related to management techniques contained in the data from Martin et al. (2018).

2.5. Calibration method

For every set of parameters that we explored, we simulated the 19 stands: the areas and sizes of the initial and final populations. We can therefore compare these values with the $19 * 4$ corresponding observations reported by Martin et al. (2018). We aimed to find a set of parameters for the plant, common to all stands, that best matches the model outputs (area and size) to field observations. Note that this compares the initial sizes of the 2008 observations and the simulated sizes. This comparison is mainly used to check if the set of parameters being tested makes it possible to obtain an initial population. Indeed, some sets of parameters can lead to a failure in the creation of populations (e.g. if the distance of competition is too great, whereas the dispersal distance is too short).

We therefore need a distance to compare the simulations and the observations. For each stand and each type (area or size), the distance: $dist(simu, data) = |simu - data|/data$ was chosen. We use a relative error distance (renormalization by the data) because areas and sizes do not have the same order of magnitude, and there is also a substantial difference within size values and area values. The total distance to minimize is the sum of the distances over the 19 stands and over the four observations (size and area, in 2008 and 2015). Note that if the set of parameters does not allow for the creation of an initial population, a population of size zero and a null area at the initial time (2008) are obtained, and the simulated values for 2015 are also null. The distance between the observations and a trivial (null) population is equal to $76 = (19 * 4)$.

To minimize this distance, the OpenMOLE software proposes a method based on genetic algorithms for model calibration (NSGA2). The result obtained is presented in Section 3.1. The calibration algorithm is an iterative algorithm, which provides a set of solutions at each step. As steps go by, the distance $dist(simu, data)$ between the data and the simulation results for the selected solutions decreases.

2.6. Numerical analysis

Simulations are performed with the set of parameters obtained by calibration (Section 3.1, Table 1).

Let us now explain how we studied the influence of the management parameters τ and T and of the initial population size, where we recall that:

- τ is the mean number of mowing events a year,
- T is the duration of the project.

We focus on the influence of these three parameters and we do not study the influence of the *proportionMowing* parameter. Its value is set at 0.9 and the random management technique is used. Indeed, we consider that the manager aims at mowing the whole stand, but we do not use a value of *proportionMowing* equal to 1 in order to consider an imperfect mowing event due to the tool used (as mentioned in Section 2.1).

Samplings of management parameters are performed in OpenMOLE, with a replication of size $n = 50$ for each set of management parameters (these samplings are detailed in Section 3.2) and the mean quantities are calculated over these n values. We first let one parameter vary. Based on an initial visual inspection of simulation results, we fit three relationships via least squares: a linear regression performed with *R* function *lm*, a truncated quadratic relationship (Equation (12)), and an exponential regression (Equation (11)) performed with *R* function *nls*. We assess model performance using the coefficient of determination (R^2) and the root mean squared errors (*RMSE*). Finally, in Section 3.2.4, we use the same statistical tools (*lm* and *nls*) to derive general regression formulas for the mean output quantities depending on management parameters, and two constants that the algorithm aims to find.

3. Results

3.1. Calibration

The values of calibrated parameters are presented in Table 1.

The set of solutions provided by the NSGA2 algorithm stabilized after 165000 steps. For a set of parameters, *evol.sample* refers to the number of replications that were carried out by the algorithm. Since the model is stochastic, we need to choose a solution with a sufficiently large value for *evol.sample* to obtain a reliable solution. Among the set of solutions provided by the algorithm, we chose the solution that was replicated at least 50 times, and that minimizes the distance $dist(simu, data)$.

Variable	Value after calibration	unit
K	12.72	g
L	0.26	$year^{-1}$
distanceCompetition	0.15	m
distanceParent	0.20	m
shape	4.34	
scale	2.36	
deathParameterDecrease	2.32	g^{-1}
deathParameterScaling	1.12	$year^{-1}$
mowingParameter	0.11	g^{-1}
bbar	0.18	$year^{-1}$
a0	1.73	g
score	26.06	
evol.sample	79	

Table 1: Result of the calibration obtained with OpenMole software (Reuillon et al., 2013)

In Table 1, *score* is the median over the 79 replications of the sum of the distances $dist(simu, data)$ over the 19 stands and the four characteristics (initial or final and area or size). A score of 26.06 means that in half of the cases and on average, the relative distance for one characteristic between the simulated stand and the corresponding data is lower than 0.3. The reason for this difference is that data were obtained from field work that was not carried out to calibrate the model, and thus may contain a bias due to the altitude or soil type.

Even though values for the plant dynamics parameters were not found in the literature, experts can provide boundaries for some of them, allowing assessment of the ecological quality of the result given by the algorithm. First, the parameters *distanceCompetition* and *distanceParent* are close to what is expected according to field experience. Then the distribution for the dispersal of individuals is close to that suggested by specialists (Figure A.1c). Figure A.1d plots the mortality rate of a crown according to its biomass. We note that a crown that is not mown keeps a very low mortality rate, in agreement with field observations. Indeed, to compare with the value in Smith et al. (2007), using Equation (8) and the parameter values from calibration, the probability that a crown dies before 4 months is calculated. This quantity is equal to 0.0027, which has the same order of magnitude as the value found in Smith et al. (2007) for the probability of a rhizome segment dying in a 4-month period (0.0083).

Finally, the ratio between the value of K (maximum biomass, that is likely to be found for the oldest crown, i.e. in the centre of the stand when there is no mowing), and a_0, the biomass of a crown at birth (rather than at the periphery) equals 7.4 (the ratio is expected to be around 10 in Adachi et al. (1996)).

3.2. Influence of management parameters and initial population size

In this section, the aim is to find statistical relationships between the explanatory variables (management parameters or initial population size) and model outputs (mean area and size of a stand).

We consider the two following samplings:

- In *sampling*1, we make τ vary in $[0, 15]$ in steps of 0.5, T in $[0, 16]$ in steps of 1 and $initialPopSize$ is set to 500 or 1500. We run 50 simulations of the stochastic model for each set of values. *sampling*1 has a high sampling rate on τ and T, with high values for the initial population size. It is used in Sections 3.2.1 and 3.2.2 to study the influence of τ and T more precisely.

- In *sampling*2, we make τ vary in $[0, 14]$ in steps of 2, T in $[0, 16]$ in steps of 2 and $initialPopSize$ in $[50, 1200]$ in steps of 50. We run 50 simulations of the stochastic model for each set of values. *sampling*2 has a high sampling rate on the initial population size. It is used in Section 3.2.3 to study its influence more precisely.

3.2.1. Influence of management duration T

In this section, the first sampling (*sampling*1) is used to study the influence of the management duration T on the final mean areas and sizes. Given τ and a value of the initial population size, we perform:

- a truncated quadratic regression for the mean final area;

- a non-linear regression on strictly positive values for the mean final population size, using the function $f(T) = initialPopSize * exp(-T/rate)$, with *rate* being a constant on which the algorithm *nls* maximizes R^2. This constant rate is different for each set of parameters, since it depends on the values of τ and $initialPopSize$. In Section 3.2.4, we study this dependency.

It turns out that for values of $\tau \leq 2.5$, the mean area remains close to its initial value at time $T = 0$ (a maximum relative difference of 3 m^2), and the variation is rather linear, but the corresponding R^2 values are below 0.9. Figure 3 gives an example of the linear regression on the mean area as a function of management duration T, for fixed given values of $\tau \leq 2.5$ and initial population size.

R^2 and *RMSE* values enable us to conclude that the mean final area depends quadratically on the management duration T when $\tau > 2.5$. Indeed, 47 regressions out of the 50 in the sampling (variation of initial Population size and $\tau > 2.5$) lead to an R^2 value larger than 0.95. The maximum value of *RMSE* over these 50 regressions is 1.31 m^2, which is low compared to the mean initial area, which has values 20 m^2 or 60 m^2. Figure 4 gives an example of the quadratic regression on the mean area as a function of management duration T for fixed given values of τ and initial population size.

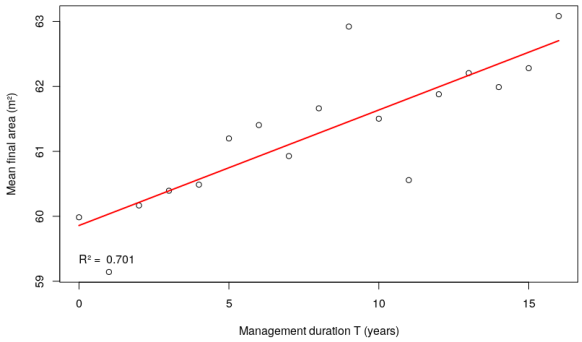

Figure 3: Linear regression of the mean final area as a function of management duration T, with $\tau = 0.5\ year^{-1}$ and $initialPopSize = 1500$.

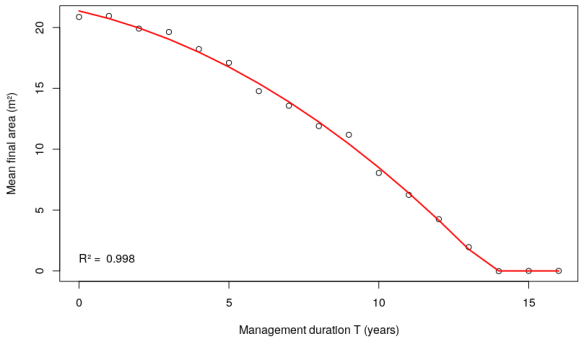

Figure 4: Quadratic regression of the mean final area as a function of management duration T, with $\tau = 8\ year^{-1}$ and $initialPopSize = 500$. For the last three points in the bottom right-hand corner, at least half of the 50 simulations lead to extinction.

These results give information on the influence of the duration of the management project on stand growth. A first fact, very important for management, is that it is not sufficient to mow to decrease the population size and area: if the number of mowings per year is too low (less than 2.5 in the present case), the population size and area increase during the management project. Figure 5 plots the quadratic regression curves for the average final area with respect to the duration of the management project (T, on the abscissa), obtained for different τ. A second important fact for management is that eradication of a knotweed stand initially covering 60 m^2 cannot be expected in less than 11 years (for 15 mowing events a year). The figure also illustrates the stand surface reduction in terms of final mean area when mowing one more time per year. For example, mowing six times a year instead of five, over 10 years, reduces the final surface of the stand by 4 m^2 on average (looking at the section $T = 10$ in Figure 5).

As for the area, the size varies linearly for values of $\tau \leq 2.5$ (R^2 around 0.9). When $\tau > 2.5$, R^2 and $RMSE$ values enable us to conclude that the mean final size depends exponentially on the management duration project T. Indeed, all 50 regressions in the sampling (variation of initial Population size and $\tau > 2.5$)

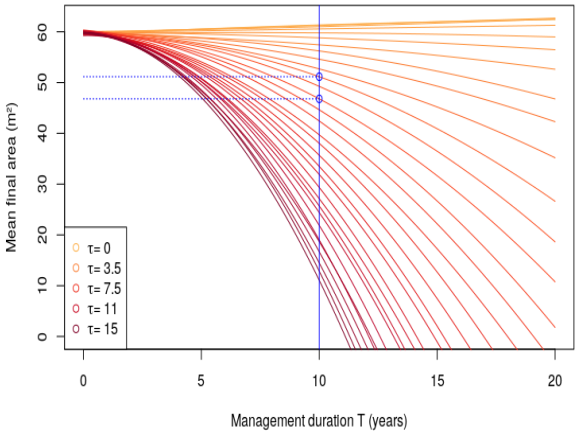

Figure 5: Quadratic regression curves of the mean final area as a function of T, for different values of τ (low in light colours, up to 15 mowings per year in dark colours), and we set $initialPopSize = 1500$ and $proportionMowing = 0.9$.

lead to an R^2 value greater than 0.95. The maximum value of $RMSE$ over these 50 regressions is 39 crowns, which is low compared to the initial population size, which has values of 500 crowns or 1500 crowns.

Figure 6 gives an example of the quadratic regression on the mean area as a function of management duration T for fixed given values of τ and the initial population size.

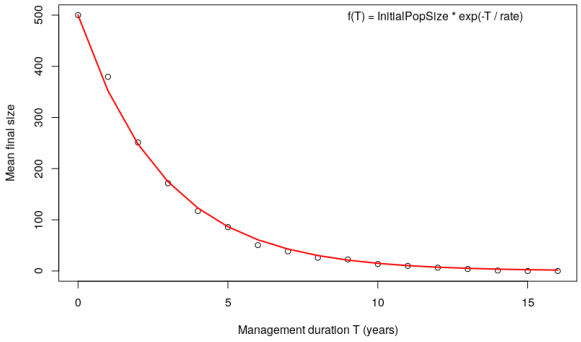

Figure 6: Non-linear regression of the mean final size as a function of management duration project T with $\tau = 8\ years^{-1}$ and initial $initialPopSize = 500$. For the last three points in the bottom right-hand corner, at least half of the 50 simulations lead to extinction.

3.2.2. *Influence of the mean number of mowing events a year τ*

In this section, we use the first sampling ($sampling1$) to study the influence of the mean number of mowing events a year on the final mean areas and sizes. Given a value of the initial population size and T, we perform:

- a linear regression on strictly positive values of outputs for the mean area;

- a non-linear regression on strictly positive values for the mean final population size, using the function $f(\tau) = initialPopSize * exp(-\tau/rate)$, with *rate* being a constant on which the algorithm *nls* minimizes the sum of squared errors. This constant rate differs for each set of parameters since it depends on the values of T and $initialPopSize$. As mentioned for the similar constant in Section 3.2.1, we study this dependency in Section 3.2.4.

The linear regression presented below holds for $\tau > 2.5$ (as in Section 3.2.1) and $T \geq 2$ (to have a decreasing population).

The R^2 and *RMSE* values enable us to conclude that the mean final area depends linearly on the mean number of mowing events τ. Indeed, 24 regressions out of the 30 in the sampling (variation of initial Population size and $T \geq 2$) lead to an R^2 value larger than 0.95. The maximum value of *RMSE* over these 50 regressions is 2.09 m^2, which is low compared to the mean initial area, which has values 20 m^2 or 60 m^2.

Figure 7 gives an example of the linear regression on the mean area as a function of the mean number of moving events for fixed given values of T and initial population size.

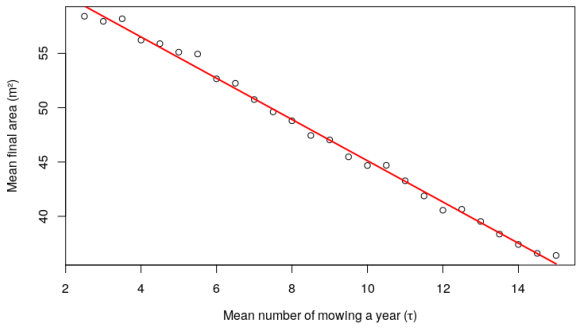

Figure 7: Linear regression of the mean final area as a function of the mean number of mowing events τ with $T = 8$ *years* and $initialPopSize = 1500$.

We also conclude that the mean final size depends exponentially on the mean number of mowing events τ. Indeed, the 30 regressions in the sampling (variation of initial Population size and $T \geq 2$) lead to an R^2 value greater than 0.95. The maximum value of *RMSE* over these 50 regressions is 64 crowns, which is low compared to the initial population size, which has values of 500 crowns or 1500 crowns.

Figure 8 gives an example of the non-linear regression on the mean size as a function of the mean number of moving events for fixed given values of T and the initial population size.

3.2.3. *Influence of the initial population size*

In this section, we use the second sampling (*sampling*2) to study the influence of the initial population size on the final mean areas and sizes. Given a value for τ and T, we perform a linear regression on strictly positive output values. Due to the wide range of values for the initial population size in the *sampling*2, too many extinctions may occur for a given set of

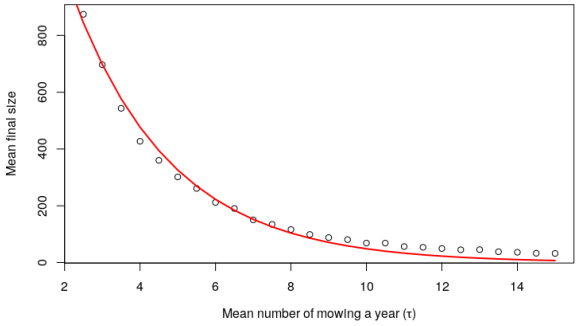

Figure 8: Non-linear regression of the mean final size as a function of the mean number of mowing events τ with $T = 8$ *years* and $initialPopSize = 1500$.

management parameters. We therefore perform the regression only if there are at least five strictly positive output values.

R^2 and *RMSE* values enable us to conclude that both the mean final area and size depend linearly on initial population size. Indeed, in both cases, 60 regressions out of the 63 regressions among the 72 management sets in the sampling lead to an R^2 value greater than 0.95. The maximum value of *RMSE* over these 63 regressions is 1.1 m^2 (resp., 18 crowns) for the mean final area (resp., size) case, which is low compared to the mean initial area (resp., initial population size), which ranges from 2 m^2 to 48 m^2 (resp., from 50 crowns to 1200 crowns).

Note that the influence of the initial population size on the initial area is also linear. Indeed, *sampling*2 contains the case $T = 0$, and for this specific value of T the final area is the initial area.

Figures 9 and 10, respectively, give an example of the linear regression on the mean size and the mean area as functions of initial population size for fixed given values of T and τ.

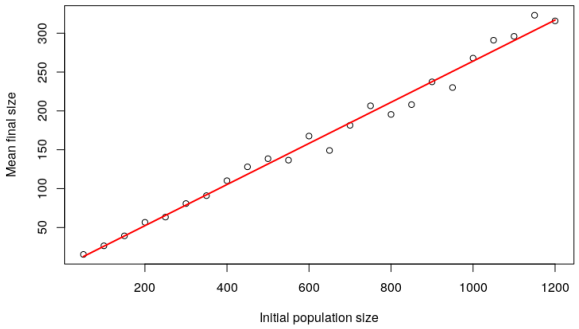

Figure 9: Linear regression of the mean final size as a function of initial population size with $T = 8$ *years* and $\tau = 4$ $years^{-1}$.

3.2.4. *Formulas for the mean final sizes and areas, as functions of τ, T and the initial population size*

We summarize results of the regressions performed in Table 2.

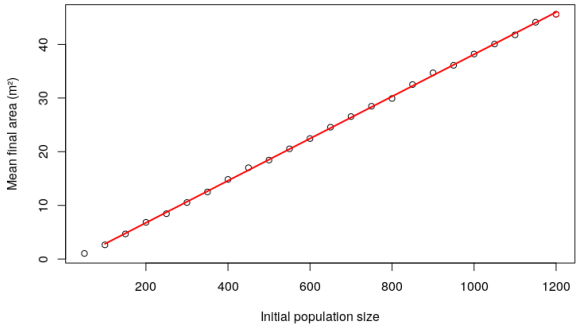

Figure 10: Linear regression of the mean final area as a function of initial population size with $T = 8$ *years* and $\tau = 4$ *years*$^{-1}$.

Parameter	Mean output	Variation	$R^2 > 0.95$	RMSE
T for $\tau \geq 2.5$	final area	quadratic ↘	47/50	1.31
T for $\tau \geq 2.5$	final size	exponential ↘	50/50	39
τ for $\tau \geq 2.5$	final area	linear ↘	24/30	2.09
τ for $\tau \geq 2.5$	final size	exponential ↘	30/30	64
initialPopSize	final area	linear ↗	60/63	1.1
initialPopSize	final size	linear ↗	60/63	18

Table 2: Summary of the regression results of Sections 3.2.1-3.2.3.

In Sections 3.2.1 to 3.2.3, we studied the influence of one parameter, while the two others were set constant. The two previous samplings introduced at the very beginning of Section 3.2 were designed to control the variation of management parameters and initial population size, in order to investigate their influence on the model outputs. Based on results in Sections 3.2.1 to 3.2.3, we are now able to propose a formula for the mean areas and sizes as a function of the two management parameters (the mean number of mowing events a year (τ) and the management project duration (T)) and the initial population size. We use a Sobol sampling (which maximizes the discrepancy of the sequence, i.e. the space is evenly covered) of 5000 points with $\tau \in [0; 15.0]$, $T \in [0; 20]$, and $initialPopSize \in [100; 1500]$.
For the same reason as before, we consider the case of $\tau \geq 2.5$. Equations (11) and (12) summarize relationships between final outputs, management parameters and initial population size:

$$Mean\ Final\ Size\ = initialPopSize * exp(-T.(\tau - a)/b), \quad (11)$$

with $a, b \in \mathbb{R}$ constants, and

$$Mean\ Final\ Area\ = \max((c \times \tau + d) * T^2 + 0.04 * initialPopSize, 0) \quad (12)$$

with $c, d \in \mathbb{R}$ constants.

We now discuss the results of the non-linear regression with respect to the two management parameters (T and $\tau \geq 2.5$) and initial population size (the sampling contains 4332 values for the triplet (T, τ, $initialPopSize$)). R^2 and $RMSE$ between the predicted values and the data for the mean size are equal to 0.99 and 26.12 crowns, respectively. The 95% confidence intervals for the constants a and b obtained with R are $a \in [0.90; 0.94]$ and $b \in [20.46; 20.77]$. R^2 and $RMSE$ between the predicted values and the data for the mean area are equal to 0.99 and 2.23 m^2, respectively. Moreover, the corresponding 95% confidence intervals for the constants c and d are $c \in [-0.0342; -0.0336]$ and $d \in [0.0960; 0.0998]$, respectively. Taking $T = 0$ in the right-hand side of Equations (11) and (12), gives $initialPopSize$ and $initialPopSize * 0.04$, respectively. The last quantity therefore corresponds to the mean initial area. There is indeed a linear dependency between the mean initial area and the initial population size.
It is important to note that the results obtained for the mean output quantities are still relevant for direct outputs. Figure 11 illustrates this point, plotting the formula (11) with T varying and for given values of τ and initial population size. We emphasize that the red line in Figure 11 was obtained with a regression on a far larger set of points than the subset selected to plot this example.

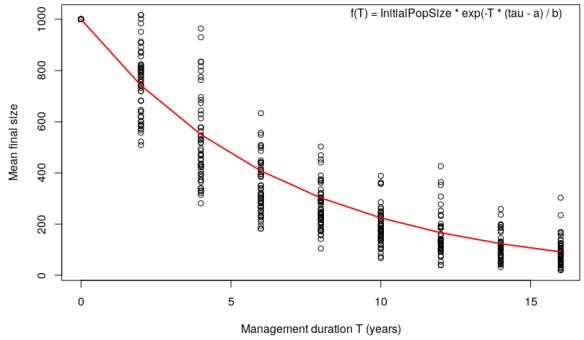

Figure 11: Exponential regression for the mean final size as a function of management duration (T). The red line is the prediction function of T defined by Equation (11). Black circles represent stand sizes resulting from 50 replications with $\tau = 4$, $initialpopulationsize = 1000$, letting T vary.

Equations (11) and (12) enable us to find which parameter most influences model outputs, and thus on which one it is better to concentrate management efforts. To do so, for each value of the triplet (T,τ,$initialPopSize$) the final size and area were compared according to Equations (11) and (12), for the three following parameter value combinations: ($T+1$,τ,$initialPopSize$), (T,$\tau+1$,$initialPopSize$) and (T,τ,$initialPopSize \times 0.9$). Each plot on Figures 12 and 13 corresponds to a fixed value of $initialPopSize$, with τ varying on the x-axis and T varying on the y-axis, and with each triplet associates the most important parameter in a management perspective, that is the parameter whose modification produces the lowest output (it is not necessarily unique). Brown zones correspond to the set of parameter values that lead to eradication; therefore, in this zone no gain can be expected from any modification. Figure 12 shows that, out of the extinction zones, T or τ has the greatest influence on final size and makes it possible to determine the most efficient management modification. Most particularly, when τ is low, it is more efficient in terms of size reduction to mow once more each year, and conversely, when T is low, it is more efficient to continue mowing 1 more year. As for the final area, we observe in Figure 13 that areas corresponding to the greatest influence

of T or τ are reduced compared to Figure 12, in favour of the area of greatest influence of *initialPopSize*. In these parameter value regions, beginning the management project on smaller stands (size equal to 90% of reference size) has a greater impact on the final area than mowing once each year or over a period of time 1 year longer; therefore, in these conditions, early detection and mowing of stands should be encouraged. Note, however, that to stop invasion, one always needs to increase both τ and T.

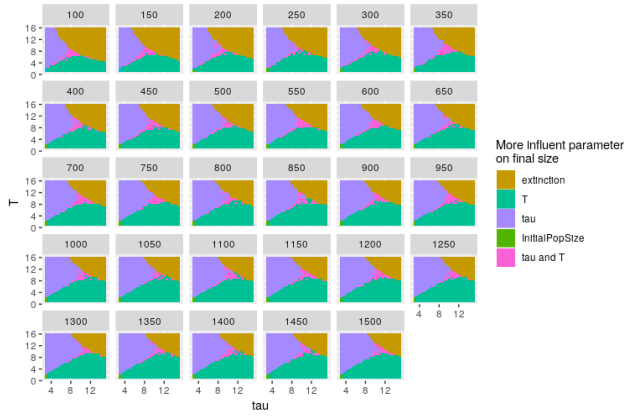

Figure 12: Parameters having the greatest influence on final size. Each plot corresponds to a fixed value of *initialPopSize* specified above the plots (from 100 to 1500 crowns), τ varies on the x-axis, and T varies on the y-axis.

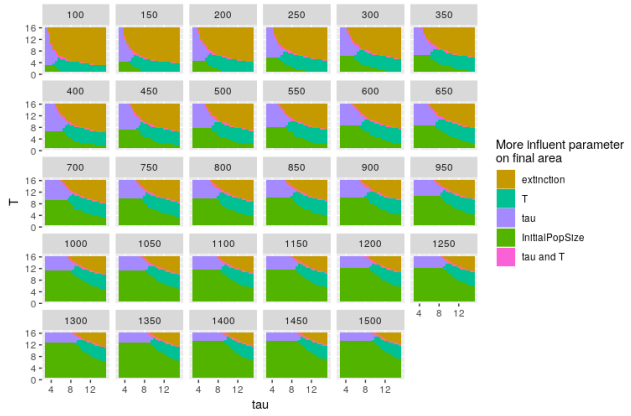

Figure 13: Parameters having the greatest influence on final area. Each plot corresponds to a fixed value of *initialPopSize* specified above the plots (from 100 to 1500 crowns), τ varies on the x-axis, and T varies on the y-axis.

4. Discussion

In this paper, we proposed a stochastic individual-based model for the growth of a stand of Japanese knotweed including mowing as a management technique. Then, we calibrated plant dynamics parameters with field data in Section 3.1. The set of parameters obtained was in agreement with values of parameters available in the literature and with our field experience. In Sections 3.2.1 - 3.2.3 we studied the influence of the initial population size, the mean number of mowing events a year and the management project duration on the mean area and size of stands. We also obtained formulas for the mean area and size of a knotweed stand, as functions of those management parameters (for $\tau > 2.5$) and initial population size. We showed that mowing once a year is not sufficient to decrease the population size and area. Indeed, if the number of mowing events per year is too low (lower than 2.5 here), the population size and area increase during the management project. We also showed how those results could be used by managers. Simulation results suggest the minimum duration of the management project necessary to achieve eradication (if it is possible at all, given a certain frequency of mowing). Figure 5 plots the quadratic regression curves for the average final area with respect to the duration of the management project (T), obtained for different values of τ and for fixed chosen values of *initialPopSize* and *proportionMowing*. The figure indicates the potential benefit, in terms of invaded area reduction, of mowing the stand once more each year. More generally, Equations (11) and (12), summarizing the relation between final outputs, management parameters and initial population size, make it possible to answer questions on the efficiency of different mowing strategies.

Following Smith et al. (2007) and Dauer and Jongejans (2013), we assumed that the invasion occurs in a homogeneous area. Models that take into account the inhomogeneity of the invaded land are often static models (no temporal component (Lookingbill et al., 2014; Buchadas et al., 2017; Hui and Richardson, 2017)). Lookingbill et al. (2014) used indices such as habitat suitability, constructed from field data such as humidity or soil type, to produce invasibility maps. These maps assign a score to each zone which describes its probability of being invaded. Invasibility (and invasiveness) in ecological networks can also be related to plant traits (Hui et al., 2016).

Another simplification in our model is that we did not take into account the dispersal of fragments of rhizome due to mowing. This may be a significant means of propagation of the plant in some conditions and it contributes to its invasiveness (Sásik and Eliás, 2006). Dispersal has to be considered if one wants to model the invasion of Japanese knotweed at the scale of a region composed of several stands. This will be the subject of future work. We could formulate this problem in the formalism of the viability theory (Aubin, 1991). In this framework, the dynamics of the system depends on the system state and on controls. One objective is to prove the existence of controls and to find initial values of the system such that the system state remains in a set of constraints (e.g. the invaded area below a given threshold). For example, managers could be interested in controlling the density of Japanese knotweed. Then we could study the resilience of the system, that is to say its ability to recover a property after a perturbation.

The importance of integration (biomass transfer between crowns) is still under debate. In Price et al. (2002), the authors note that there is relatively little integration, whereas in Suzuki (1994) the authors found greater integration. We did not consider this process in the model. Adding this phenomenon could produce simulation results closer to reality.

The field data we used for the calibration were extracted from Martin et al. (2018). The measurements were taken in 2008 and

2015 on stands that were mown or not mown. For each stand, data provide information on the management technique used by the land owner: the frequency of mowing and an estimation of the proportion of the mown stand. Calibration results for some of the plant dynamics parameters based on these measurements are in agreement with data found in the literature.
The model is written in the formalism of measure-valued stochastic processes. The tools we used here in the case of a Japanese knotweed stand may be used by practitioners to test for different management options (such as one-side mowing) and objectives (containment or eradication). Moreover, they can also be used in a more general context. In particular, we could apply this method to other invasive plants, such as seed dispersal species. One could even allow individuals to move in such models. In Leman (2016), the author took into account the spatial motion in an individual-based stochastic population model. Furthermore, including sexual reproduction of individuals, as in Smadi et al. (2018), would also enable one to consider animal invasive species, such as mosquitoes (Juliano and Philip Lounibos, 2005) or feral cats (Baker and Bode, 2016).

Aknowledgements

This work was partially funded by Electricité De France (EDF) and we thank Laure Santoni and Agnes Bariller for helpful discussions and comments. FL, SM and CS acknowledge partial funding from the Chair "Modélisation Mathématique et Biodiversité" of VEOLIA-Ecole Polytechnique-MNHN-F.X. FL and BR also acknowledge partial funding through the ANR "Alien" project (ANR 14-CE36-0001-01). Finally, IA, FL, SM and CS acknowledge Complex System Institute of Paris Île-de-France for hosting, and the OpenMOLE team for their advice on the software.

Appendix A. Summary of model parameters

Table A.1 summarizes the plant dynamic parameters. We specify parameter units for those that have a biological meaning.

Variable	Description	Unit
Biomass		
K	maximum biomass (Equation (7))	g
L	biomass growth rate for low biomass (Equation (7))	$year^{-1}$
a_0	initial biomass (of a crown at birth)	g
Mowing		
mowingParameter	in the mowing effect function in Equation (5)	g^{-1}
Mortality		
deathParameterScaling	mortality rate for the low biomasses in Equation (9)	$year^{-1}$
deathParameterDecrease	decay rate of mortality function in Equation (9)	g^{-1}
Birth		
distanceParent	apical dominance distance (Equation (1))	m
distanceCompetition	intra-specific competition distance (Equation (4))	m
$\bar{b}$	birth rate (under ideal conditions)	$year^{-1}$
(shape, scale)	Gamma law, dispersion of new individual	

Table A.1: Summary of model parameters

We have the following management parameters:

- mean number of mowing events a year: τ;
- management project duration: T;
- proportion of mown crowns: *proportionMowing*;

and initial population size parameter: *initialPopSize*.

Appendix B. Description of the algorithm used to simulate a solution of Equation (10).

We present one step of Gillespie's algorithm used to simulate the stand dynamics. Three types of events may occur: a birth, a death or the mowing of a proportion *proportionMowing* of individuals in the population. Suppose we have N individuals at a time t. We start by calculating the time of the next event, which requires the sum of the birth, death and mowing event rates. The law of this time only depends on the current population state given that the process is Markovian.
If it is a birth event, we select the parent uniformly at random in the population. We check whether the individual selected to be the parent does not already have too many neighbours at a distance lower than *distanceParent*. If this occurs, we draw the position of the new individual (child) according to the Gamma law described in "Dispersal of the newborn individual" of Section 2.1 (with an angle chosen uniformly around the potential parent). If the child's position falls into the set C of Equation (4) (i.e. it does not fall into an intra-specific competition zone), then the individual is born at this position, and the new population size is $N + 1$. Otherwise, i.e. if the parent has already enough crowns close to it, or if the new individual to be born is out of the set C, then there is no birth, and the population size remains N.
If the event is a mowing event, then we mow every individual with probability *proportionMowing*: we replace its biomass a by $a * F(a)$.
Finally, if the event is a death event, then the individual likely to die is drawn uniformly at random, and we choose with the realization of a random variable whether this individual really dies according to its mortality rate, which depends on its biomass. If it dies, it is taken out of the population and the new population size is $N - 1$; otherwise, nothing happens.
Between two events, the biomass of each individual grows in a deterministic way. The algorithm stops as soon as there are no more individuals in the population.

For the simulations, we have to specify an initial population (at time 0, positions and biomass) that will evolve. To create an initial population, we use the algorithm above with initially one individual until the population reaches a prescribed size, with a low management technique ($\tau = 1$ and $proportionMowing = 0.9$). Indeed, if we put a higher value of τ, we cannot often create the initial population because the original individual dies before producing offspring. In this spirit, we also allow several attempts in the algorithm to create the initial population.

Appendix C. Plots of functions defined in Section 2.1 with plant dynamics parameters from the calibration

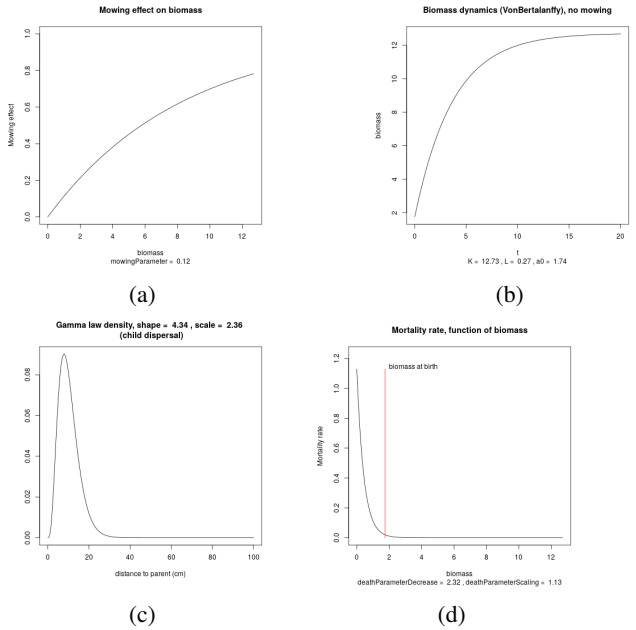

Figure A.1: Plots of functions defined in Section 2.1 with plant dynamics parameters from the calibration.
Figure A.1a: Function for the effect of mowing, Equation (5) with parameter values from the calibration (Table 1).
Figure A.1b: Biomass dynamics of an individual, with no mowing events for 20 years (Equation (7)) with parameter values from the calibration (Table 1).
Figure A.1c: Gamma law for the distance of dispersion with parameter values from the calibration (Table 1).
Figure A.1d: Mortality rate, as a function of biomass (Equation (9)) with parameter values from the calibration (Table 1).

References

Abgrall, C., Forey, E., Mignot, L., Chauvat, M., 2018. Invasion by *Fallopia japonica* alters soil food webs through secondary metabolites. Soil Biology and Biochemistry 127, 100–109.

Adachi, I., Naoki, T., Terashima, M., 1996. Central die-back of monoclonal stands of *Reynoutria japonica* in an early stage of primary succession on Mount Fuji. Annals of Botany 77, 477–486.

Alberternst, B., Böhmer, H., 2006. Invasive alien species fact sheet- *Fallopia japonica*-. online database of the North European and Baltic network on invasive alien species-nobanis. www. nobanis. org .

Aubin, J.P., 1991. Viability theory. Springer Science & Business Media.

Bailey, J., Wisskirchen, R., 2006. The distribution and origins of *Fallopia* × *bohemica* (Polygonaceae) in europe. Nordic Journal of Botany 24, 173–199.

Bailey, J.P., Bímová, K., Mandák, B., 2009. Asexual spread versus sexual reproduction and evolution in Japanese knotweed *s.l.* sets the stage for the "battle of the clones". Biological Invasions 11, 1189–1203.

Baker, C.M., Bode, M., 2016. Placing invasive species management in a spatiotemporal context. Ecological Applications 26, 712–725.

Barney, J.N., Tharayil, N., DiTommaso, A., Bhowmik, P.C., 2006. The biology of invasive alien plants in Canada. 5. *Polygonum cuspidatum* Sieb. & Zucc.[= *Fallopia Japonica* (Houtt.) Ronse Decr.]. Canadian Journal of Plant Science 86, 887–906.

Bashtanova, U.B., Beckett, K.P., Flowers, T.J., 2009. Physiological approaches to the improvement of chemical control of Japanese knotweed (*Fallopia japonica*). Weed science 57, 584–592.

Beerling, D.J., Bailey, J.P., Conolly, A.P., 1994. *Fallopia japonica* (Houtt.) Ronse Decraene. Journal of Ecology 82, 959–979.

von Bertalanffy, L., 1934. Untersuchungen über die gesetzlichkeit des wachstums. Wilhelm Roux'Archiv für Entwicklungsmechanik der Organismen 131, 613–652.

Bolker, B., Pacala, S.W., 1997. Using moment equations to understand stochastically driven spatial pattern formation in ecological systems. Theoretical Population Biology 52, 179–197.

Bonneau, M., Martin, J., Peyrard, N., Rodgers, L., Romagosa, C.M., Johnson, F.A., 2019. Optimal spatial allocation of control effort to manage invasives in the face of imperfect detection and misclassification. Ecological modelling 392, 108–116.

Brock, J., Wade, M., et al., 1992. Regeneration of Japanese knotweed (*Fallopia japonica*) from rhizomes and stems: observation from greenhouse trials., in: IXe Colloque international sur la biologie des mauvaises herbes, 16-18 September 1992, Dijon, France., ANPP. pp. 85–94.

Buchadas, A., Vaz, A.S., Honrado, J.P., Alagador, D., Bastos, R., Cabral, J.A., Santos, M., Vicente, J.R., 2017. Dynamic models in research and management of biological invasions. Journal of Environmental Management 196, 594–606.

Cacho, O.J., Hester, S., Spring, D., 2007. Applying search theory to determine the feasibility of eradicating an invasive population in natural environments. Australian Journal of Agricultural and Resource Economics 51, 425–443.

Cacho, O.J., Spring, D., Hester, S., Mac Nally, R., 2010. Allocating surveillance effort in the management of invasive species: a spatially-explicit model. Environmental Modelling & Software 25, 444–454.

Champagnat, N., 2006. A microscopic interpretation for adaptive dynamics trait substitution sequence models. Stochastic Processes and their Applications 116, 1127–1160.

Champagnat, N., Ferrière, R., Méléard, S., 2006. Unifying evolutionary dynamics: from individual stochastic processes to macroscopic models. Theoretical Population Biology 69, 297–321.

Colleran, B.P., Goodall, K.E., 2014. In situ growth and rapid response management of flood-dispersed Japanese knotweed (*Fallopia japonica*). Invasive Plant Science and Management 7, 84–92.

Coron, C., Costa, M., Leman, H., Smadi, C., 2018. A stochastic model for speciation by mating preferences. Journal of Mathematical Biology 76, 1421–1463.

Costa, M., Hauzy, C., Loeuille, N., Méléard, S., 2016. Stochastic eco-evolutionary model of a prey-predator community. Journal of Mathematical Biology 72, 573–622.

Dassonville, N., Guillaumaud, N., Piola, F., Meerts, P., Poly, F., 2011. Niche construction by the invasive Asian knotweeds (species complex *Fallopia*): impact on activity, abundance and community structure of denitrifiers and nitrifiers. Biological Invasions 13, 1115–1133.

Dauer, J.T., Jongejans, E., 2013. Elucidating the population dynamics of Japanese knotweed using integral projection models. PloS one 8, e75181.

De Waal, L., 2001. A viability study of *Fallopia japonica* stem tissue. Weed Research 41, 447–460.

Dieckmann, U., Law, R., Metz, J.A., 2000. The geometry of ecological interactions: simplifying spatial complexity. Cambridge University Press.

Dommanget, F., Evette, A., Spiegelberger, T., Gallet, C., Pace, M., Imbert, M., Navas, M.L., 2014. Differential allelopathic effects of Japanese knotweed on willow and cottonwood cuttings used in riverbank restoration techniques. Journal of Environmental Management 132, 71–78.

Fournier, N., Méléard, S., 2004. A microscopic probabilistic description of a locally regulated population and macroscopic approximations. The Annals of Applied Probability 14, 1880–1919.

Gerber, E., Krebs, C., Murrell, C., Moretti, M., Rocklin, R., Schaffner, U., 2008. Exotic invasive knotweeds (*Fallopia spp.*) negatively affect native plant and invertebrate assemblages in European riparian habitats. Biological Conservation 141, 646–654.

Gerber, E., Murrell, C., Krebs, C., Bilat, J., Schaffner, U., 2010. Evaluating non-chemical management methods against invasive exotic knotweeds, *Fallopia Spp*. CABI, Egham .

Gourley, S.A., Li, J., Zou, X., 2016. A mathematical model for biocontrol of the invasive weed *Fallopia japonica*. Bulletin of Mathematical Biology 78, 1678–1702.

Gowton, C., Budsock, A., Matlaga, D., 2016. Influence of disturbance on Japanese knotweed (*Fallopia japonica*) stem and rhizome fragment recruitment success within riparian forest understory. Natural Areas Journal 36, 259–267.

Harris, C.M., Park, K.J., Atkinson, R., Edwards, C., Travis, J., 2009. Invasive species control: incorporating demographic data and seed dispersal into a management model for *Rhododendron ponticum*. Ecological Informatics 4, 226–233.

Hester, S., Brooks, S., Cacho, O., Panetta, F., 2010. Applying a simulation model to the management of an infestation of *Miconia calvescens* in the wet tropics of Australia. Weed Research 50, 269–279.

Hui, C., Richardson, D.M., 2017. Invasion dynamics. Oxford University Press.

Hui, C., Richardson, D.M., Landi, P., Minoarivelo, H.O., Garnas, J., Roy, H.E., 2016. Defining invasiveness and invasibility in ecological networks. Biological Invasions 18, 971–983.

Juliano, S.A., Philip Lounibos, L., 2005. Ecology of invasive mosquitoes: effects on resident species and on human health. Ecology Letters 8, 558–574.

Kettunen, M., Genovesi, P., Gollasch, S., Pagad, S., Starfinger, U., ten Brink, P., Shine, C., 2009. Technical support to EU strategy on invasive alien species (ias). London: Institut for European Environnemental Policy (IEEP) .

Landi, P., Vonesh, J.R., Hui, C., 2018. Variability in life-history switch points across and within populations explained by adaptive dynamics. Journal of the Royal Society Interface 15, 20180371.

Lavoie, C., 2017. The impact of invasive knotweed species (*Reynoutria spp.*) on the environment: review and research perspectives. Biological Invasions 19, 2319–2337.

Leman, H., 2016. Convergence of an infinite dimensional stochastic process to a spatially structured trait substitution sequence. Stochastics and Partial Differential Equations: Analysis and Computations 4, 791–826.

Lookingbill, T.R., Minor, E.S., Bukach, N., Ferrari, J.R., Wainger, L.A., 2014. Incorporating risk of reinvasion to prioritize sites for invasive species management. Natural Areas Journal 34, 268–281.

Maerz, J.C., Blossey, B., Nuzzo, V., 2005. Green frogs show reduced foraging success in habitats invaded by Japanese knotweed. Biodiversity & Conservation 14, 2901–2911.

Martin, F.M., Dommanget, F., Janssen, P., Spiegelberger, T., Viguier, C., Evette, A., 2018. Could knotweeds invade mountains in their introduced range? An analysis of patches dynamics along an elevational gradient. Alpine Botany .

Meier, E.S., Dullinger, S., Zimmermann, N.E., Baumgartner, D., Gattringer, A., Hülber, K., 2014. Space matters when defining effective management for invasive plants. Diversity and Distributions 20, 1029–1043.

Murphy, G.E., Romanuk, T.N., 2014. A meta-analysis of declines in local species richness from human disturbances. Ecology and Evolution 4, 91–103.

Paine, C., Marthews, T.R., Vogt, D.R., Purves, D., Rees, M., Hector, A., Turnbull, L.A., 2012. How to fit nonlinear plant growth models and calculate growth rates: an update for ecologists. Methods in Ecology and Evolution 3, 245–256.

Panetta, F.D., Cacho, O., Hester, S., Sims-Chilton, N., Brooks, S., 2011. Estimating and influencing the duration of weed eradication programmes. Journal of Applied Ecology 48, 980–988.

Pimentel, D., Zuniga, R., Morrison, D., 2005. Update on the environmental and economic costs associated with alien-invasive species in the United States. Ecological Economics 52, 273–288.

Price, E.A., Gamble, R., Williams, G.G., Marshall, C., 2002. Seasonal patterns of partitioning and remobilization of 14C in the invasive rhizomatous perennial Japanese knotweed (*Fallopia japonica* (Houtt.) Rronse Decraene). Ecology and Evolutionary Biology of Clonal Plants , 125–140.

Pyšek, P., Richardson, D.M., 2010. Invasive species, environmental change and management, and health. Annual Review of Environment and Resources 35.

Reuillon, R., Leclaire, M., Rey-Coyrehourcq, S., 2013. Openmole, a workflow engine specifically tailored for the distributed exploration of simulation models. Future Generation Computer Systems 29, 1981 – 1990. URL: `http://www.openmole.org/files/FGCS2013.pdf`.

Rouifed, S., Bornette, G., Mistler, L., Piola, F., 2011. Contrasting response to clipping in the Asian knotweeds *Fallopia japonica* and *Fallopia* × *bohemica*. Ecoscience 18, 110–114.

Saldaña, A., Fuentes, N., Pfanzelt, S., 2009. *Fallopia japonica* (Houtt.) Ronse Decraene. (Polygonaceae), : A new record for the alien flora of Chile. Gayana. Botánica 66, 283–285.

Sásik, R., Eliás, P., 2006. Rhizome regeneration of *Fallopia Japonica* (Japanese knotweed)(Houtt.) Ronse Decr. i. regeneration rate and size of regenerated plants. Folia Oecologica 33, 57.

Seiger, L.A., Merchant, H.C., et al., 1997. Mechanical control of Japanese knotweed (*Fallopia japonica* [Houtt.] Ronse Decraene): Effects of cutting regime on rhizomatous reserves. Natural Areas Journal 17, 341–345.

Serniak, L.T., Corbin, C.E., Pitt, A.L., Rier, S.T., 2017. Effects of Japanese knotweed on avian diversity and function in riparian habitats. Journal of Ornithology 158, 311–321.

Shackleton, R.T., Shackleton, C.M., Kull, C.A., 2019. The role of invasive alien species in shaping local livelihoods and human well-being: A review. Journal of Environmental Management 229, 145–157.

Siemens, T.J., Blossey, B., 2007. American Journal of Botany 94, 776–783.

Simberloff, D., Martin, J.L., Genovesi, P., Maris, V., Wardle, D.A., Aronson, J., Courchamp, F., Galil, B., García-Berthou, E., Pascal, M., et al., 2013. Impacts of biological invasions: what's what and the way forward. Trends in Ecology & Evolution 28, 58–66.

Smadi, C., Leman, H., Llaurens, V., 2018. Looking for the right mate in diploid species: How does genetic dominance affect the spatial differentiation of a sexual trait? Journal of Theoretical Biology 447, 154–170.

Smith, J., Ward, J.P., Child, L.E., Owen, M., 2007. A simulation model of rhizome networks for *Fallopia japonica* (Japanese knotweed) in the United Kingdom. Ecological Modelling 200, 421–432.

Strayer, D.L., 2012. Eight questions about invasions and ecosystem functioning. Ecology Letters 15, 1199–1210.

Suzuki, J.I., 1994. Growth dynamics of shoot height and foliage structure of a rhizomatous perennial herb, *Polygonum cuspidatum*. Annals of Botany 73, 629–638.

Tharayil, N., Alpert, P., Bhowmik, P., Gerard, P., 2013. Phenolic inputs by invasive species could impart seasonal variations in nitrogen pools in the introduced soils: a case study with *Polygonum cuspidatum*. Soil Biology and Biochemistry 57, 858–867.

Tran, V.C., 2006. Modèles particulaires stochastiques pour des problèmes d'évolution adaptative et pour l'approximation de solutions statistiques. Ph.D. thesis. Université de Nanterre-Paris X.

Tran, V.C., 2008. Large population limit and time behaviour of a stochastic particle model describing an age-structured population. ESAIM: Probability and Statistics 12, 345–386.

Travis, J.M., Harris, C.M., Park, K.J., Bullock, J.M., 2011. Improving prediction and management of range expansions by combining analytical and individual-based modelling approaches. Methods in Ecology and Evolution 2, 477–488.

Zeide, B., 1993. Analysis of growth equations. Forest science 39, 594–616.